

Dear Author,

Please, note that changes made to the HTML content will be added to the article before publication, but are not reflected in this PDF.

Note also that this file should not be used for submitting corrections.

**AUTHOR QUERY FORM**

	<b>Journal: FOCH</b>  <b>Article Number: 16146</b>	<b>Please e-mail or fax your responses and any corrections to:</b>  <b>E-mail: <a href="mailto:corrections.esch@elsevier.sps.co.in">corrections.esch@elsevier.sps.co.in</a></b>  <b>Fax: +31 2048 52799</b>
---	--	---

Dear Author,

Please check your proof carefully and mark all corrections at the appropriate place in the proof (e.g., by using on-screen annotation in the PDF file) or compile them in a separate list. Note: if you opt to annotate the file with software other than Adobe Reader then please also highlight the appropriate place in the PDF file. To ensure fast publication of your paper please return your corrections within 48 hours.

For correction or revision of any artwork, please consult <http://www.elsevier.com/artworkinstructions>.

Any queries or remarks that have arisen during the processing of your manuscript are listed below and highlighted by flags in the proof. Click on the 'Q' link to go to the location in the proof.

<b>Location in article</b>	<b>Query / Remark: <a href="#">click on the Q link to go</a> Please insert your reply or correction at the corresponding line in the proof</b>
<a href="#">Q1</a>	Please confirm that given name(s) and surname(s) have been identified correctly.
<a href="#">Q2</a>	The decimal comma has been changed to a decimal point in sentences “Polyamide MN-SC-6...” and “using a gradient of...”. Please check, and correct if necessary.
<a href="#">Q3</a>	Please check the hierarchy of the section headings.
<a href="#">Q4</a>	Part label ‘C’ is missing in Fig. 4 artwork. Please check.
	<div data-bbox="416 1853 979 1953" style="border: 1px solid black; padding: 5px;"> <p style="color: red;">Please check this box if you have no corrections to make to the PDF file</p> <input data-bbox="868 1868 940 1932" type="checkbox"/> </div>

Thank you for your assistance.

---

**Highlights**

---

- We have studied the binding of coffee chlorogenic derivatives to human albumin.
  - Both chlorogenic acids and quinides bind strongly to Sudlow site 1 of albumin.
  - Multiple interactions are established by a dicaffeoyl quinide, with nanomolar affinity.
  - Warfarin, a reference drug binding to human albumin is displaced from the protein by low concentrations of a quinide.
- 

OF



Contents lists available at ScienceDirect

Food Chemistry

journal homepage: [www.elsevier.com/locate/foodchem](http://www.elsevier.com/locate/foodchem)

## Interaction of chlorogenic acids and quinides from coffee with human serum albumin

Valentina Sinisi<sup>a,\*</sup>, Cristina Forzato<sup>a</sup>, Nicola Cefarin<sup>a</sup>, Luciano Navarini<sup>b</sup>, Federico Berti<sup>a,\*</sup><sup>a</sup> Dipartimento di Scienze Chimiche e Farmaceutiche, Università degli Studi di Trieste, via L. Giorgieri 1, 34127 Trieste, Italy<sup>b</sup> illycaffè S.p.A., via Flavia 110, 34147 Trieste, Italy

### ARTICLE INFO

#### Article history:

Received 10 February 2014

Received in revised form 11 June 2014

Accepted 15 July 2014

Available online xxx

#### Keywords:

Human serum albumin

Protein–ligand interaction

Fluorescence spectroscopy

Coffee polyphenols

Chlorogenic acids

### ABSTRACT

Chlorogenic acids and their derivatives are abundant in coffee and their composition changes between coffee species. Human serum albumin (HSA) interacts with this family of compounds with high affinity. We have studied by fluorescence spectroscopy the specific binding of HSA with eight compounds that belong to the coffee polyphenols family, four acids (caffeic acid, ferulic acid, 5-*O*-caffeoyl quinic acid, and 3,4-dimethoxycinnamic acid) and four lactones (3,4-*O*-dicafeoyl-1,5- $\gamma$ -quinide, 3-*O*-[3,4-(dimethoxy)cinnamoyl]-1,5- $\gamma$ -quinide, 3,4-*O*-bis[3,4-(dimethoxy)cinnamoyl]-1,5- $\gamma$ -quinide, and 1,3,4-*O*-tris[3,4-(dimethoxy)cinnamoyl]-1,5- $\gamma$ -quinide), finding dissociation constants of the albumin–chlorogenic acids and albumin–quinides complexes in the micromolar range, between 2 and 30  $\mu$ M. Such values are comparable with those of the most powerful binders of albumin, and more favourable than the values obtained for the majority of drugs. Interestingly in the case of 3,4-*O*-dicafeoyl-1,5- $\gamma$ -quinide, we have observed the entrance of two ligand molecules in the same binding site, leading up to a first dissociation constant even in the hundred nanomolar range, which is to our knowledge the highest affinity ever observed for HSA and its ligands. The displacement of warfarin, a reference drug binding to HSA, by the quinide has also been demonstrated.

© 2014 Published by Elsevier Ltd.

## 1. Introduction

Phenolic acids are found as secondary metabolites in leaves, roots and especially fruits of many plants. Chlorogenic acids (CGAs) derive from the esterification with *D*-(-)-quinic acid **1** of certain cinnamic acids, such as caffeic acid **2**, ferulic acid **3** and *p*-coumaric acid **4** (Fig. 1), constituting a large family of different molecules in the form of mono- or multi-esters (Clifford, 2000).

Of all the CGAs present in green coffee beans, which are the best source of CGAs found in plants with an amount of 5–12 g/100 g (Farah, Monteiro, Donangelo, & Lafay, 2008), caffeoylquinic acids (CQAs) represent the main subgroup and 5-*O*-caffeoylquinic acid **5** (5-CQA, Fig. 1) is the most abundant one, indeed it is usually called *chlorogenic acid*. A difference between the two types of coffee was also evidenced since Robusta green coffee turned out to be richer in CGAs than Arabica (Farah, de Paulis, Trugo, & Martin,

2005). The roasting process causes a partial loss of CGAs, due to the occurrence of many reactions including isomerization, degradation, dehydration and lactonization (Fig. 1) (Clifford, 1985; Scholz & Maier, 1990; Schrader, Kiehne, Engelhardt, & Maier, 1996). The latter reaction leads to chlorogenic acid lactones (CGLs) which have also shown potential biological activities (de Paulis et al., 2002).

CGAs and CGLs are extracted during coffee brewing, and their content in the cup depend on the type of roasted coffee used and on the extraction method (Gloess et al., 2013); in a traditional *espresso* coffee beverage (30 ml) the content of monocaffeoyl quinic acids is on average 70 mg (Navarini et al., 2008). The extraction efficiency is higher for CGAs than for CGLs, due to their better water solubility, and in general a *lungo* (about 120 ml) is more rich in CGAs than a regular *espresso* coffee.

Many studies reported that polyphenols are capable to permeate the gastrointestinal barrier and are absorbed in humans, being found in plasma as both intact molecules and as their hydrolysis metabolites, in particular as caffeic acid (Farah et al., 2008; Monteiro, Farah, Perrone, Trugo, & Donangelo, 2007; Nardini, Cirillo, Natella, & Scaccini, 2002; Olthof, Hollman, & Katan, 2001; Renouf et al., 2010); CQAs have been detected in plasma even 4 h after the ingestion.

Abbreviations: CGAs, chlorogenic acids; CQAs, caffeoylquinic acids; 5-CQA, 5-*O*-caffeoylquinic acid; CQLs, chlorogenic acid lactones; DMSO, dimethyl sulfoxide; HSA, human serum albumin; Trp, tryptophan.

\* Corresponding authors. Tel.: +39 040 5583920; fax: +39 0405583903.

E-mail addresses: [valentina.sinisi@phd.units.it](mailto:valentina.sinisi@phd.units.it) (V. Sinisi), [fberti@units.it](mailto:fberti@units.it) (F. Berti).

<http://dx.doi.org/10.1016/j.foodchem.2014.07.080>  
0308-8146/© 2014 Published by Elsevier Ltd.

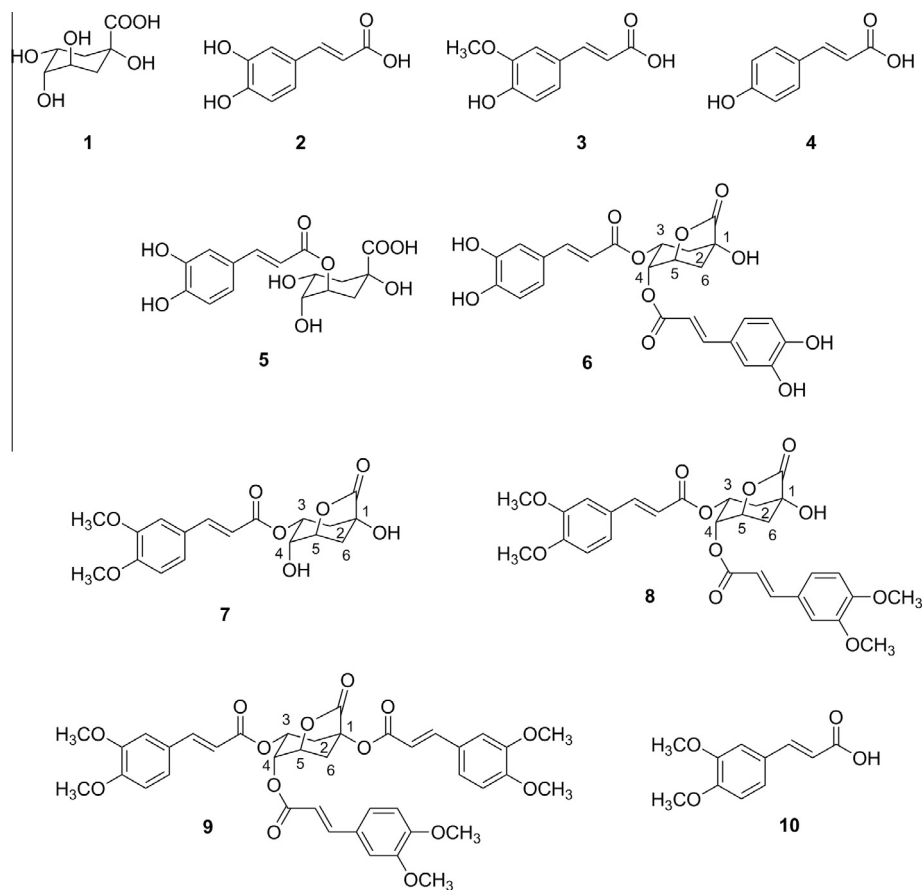


**Fig. 1.** Molecular structure of (-)-quinic acid (1), caffeic acid (2), ferulic acid (3), *p*-coumaric acid (4), 5-*O*-caffeoylquinic acid (5) (the IUPAC numbering system for chlorogenic acid (IUPAC, 1976) is adopted and, to avoid confusion, the same numbering system of the carbon atoms both for lactones and for the acid precursors is used), 3,4-*O*-dicaffeoyl-1,5- $\gamma$ -quinide (6), 3-*O*-[3,4-(dimethoxy)cinnamoyl]-1,5- $\gamma$ -quinide (7), 3,4-*O*-bis[3,4-(dimethoxy)cinnamoyl]-1,5- $\gamma$ -quinide (8), 1,3,4-*O*-tris[3,4-(dimethoxy)cinnamoyl]-1,5- $\gamma$ -quinide (9) and 3,4-dimethoxycinnamic acid (10).

84 Human serum albumin (HSA) is the most abundant protein in  
85 human plasma, a monomeric 585-residue protein containing three  
86 homologous helical domains (I–III), each divided into two subdo-  
87 mains (A and B) (He & Carter, 1992). Two main binding sites for  
88 small organic molecules are found, one located in subdomain IIA  
89 and one in IIIA, that are known as Sudlow I and Sudlow II sites,  
90 respectively (Sudlow, Birkett, & Wade, 1975a).

91 The protein is able to bind a large variety of endogenous ligands,  
92 as non-esterified fatty acids, bilirubin, heme, thyroxine, bile acids;  
93 many drugs with acidic or electronegative moieties (including phe-  
94 nols as paracetamol) also exploit the interaction with HSA to be  
95 carried in human body (Ghuman et al., 2005; Varshney et al.,  
96 2010). Recently an interactive association of multiple ligands with  
97 the same binding site inside subdomain II of HSA has been pro-  
98 posed (Yang et al., 2012). As to the binding of phenolic compounds  
99 from dietary sources, flavonoids as flavanol, flavonol, flavone, iso-  
100 flavone, flavanones, and anthocyanidins are known to interact with  
101 HSA (Pal & Saha, 2014). The interactions of catechins [(–)-epigallo-  
102 catechin-3-gallate, (–)-epigallocatechin, (–)-epicatechin-3-gallate],  
103 flavones (kaempferol, kaempferol-3-glucoside, quercetin, naringe-  
104 nin) and hydroxycinnamic acids (rosmarinic acid, caffeic acid,  
105 *p*-coumaric acid) with bovine albumin has been reported in this  
106 journal by Skrt, Benedik, Podlipnik, and Ulrich (2012). Resveratrol  
107 binds to HSA and its interaction is modulated by stearic acid  
108 (Pantusa, Sportelli, & Bartucci, 2012). Specific binding of caffeic,  
109 ferulic, and 5-CQA acids inside Sudlow site I of HSA has been stud-  
110 ied, revealing  $K_D$  about 6  $\mu$ M, 40  $\mu$ M and 25  $\mu$ M respectively (Kang

et al., 2004; Min et al., 2004; Hu, Chen, Zhou, Bai, & Ou-Yang,  
2012). In this study the aim was to extend the knowledge regard-  
ing the interaction between polyphenols present in coffee and HSA.  
For this purpose we have synthesised four quinides of caffeic acid  
and of 3,4-*O*-dimethoxycinnamoyl acid: 3,4-*O*-dicaffeoyl-1,5- $\gamma$ -  
quinide **6**, 3-*O*-[3,4-(dimethoxy)cinnamoyl]-1,5- $\gamma$ -quinide **7**, 3,  
4-*O*-bis [3,4-(dimethoxy)cinnamoyl]-1,5- $\gamma$ -quinide **8**, and 1,3,  
4-*O*-tris [3,4-(dimethoxy)cinnamoyl]-1,5- $\gamma$ -quinide **9** (Fig. 1).

Compound **6** is very abundant in roasted coffee, while the class  
of dimethoxycinnamoylquinic acids, precursors of compounds **7**, **8**,  
and **9**, was recently found and characterised in green coffee beans  
(Clifford, Knight, Surucu, & Kuhnert, 2006).

We have measured the dissociation constants to Sudlow site I of  
our compounds in physiological conditions by fluorescence spec-  
troscopy following the quenching of the emission of the unique  
fluorescent tryptophan residue within the binding site in subdo-  
main IIA (Trp-214) (Anna, 2002).

The absorption, distribution, albumin binding and excretion of  
phenolic derivatives **10** in human plasma after coffee consumption  
have been studied, but more complex derivatives were not consid-  
ered yet (Farrell et al., 2012; Nagy et al., 2011). Our data may  
therefore be interesting to better understand the effects of coffee  
consumption on the human body, as to the binding to albumin  
and potential competition with drugs at the same site. Moreover,  
we are also interested in the development of biosensing tools for  
the rapid detection of coffee polyphenols in quality control of cof-  
fee beverages. HSA could represent a valuable binder to be used in

such analytical devices for capturing coffee polyphenols. We have recently obtained a functional 100 aminoacid fragment of HSA, to be used as the starting scaffold to generate a library of albumin-derived binders with improved affinity and selectivity (Luigi et al., 2013).

## 2. Materials and methods

### 2.1. Materials

HSA essentially fatty acid free (A3782, ~99%), caffeic acid ( $\geq 98\%$ ), ferulic acid (99%), 3,4-dimethoxy cinnamic acid (predominantly *trans*, 99%), chlorogenic acid hemihydrate ( $\geq 98\%$ ) and all the reagents for the synthesis were purchased from Sigma–Aldrich Co. (St. Louis, MO, USA) and used without further purification. Polyamide MN-SC-6 0.05–0.16 mm was purchased from Mache-rey–Nagel (Düren, Germany).

### 2.2. Apparatus

Melting points were measured on a Sanyo Gallenkamp apparatus; the optical activity measurements ( $[\alpha]$ ) were performed with a Perkin–Elmer 241 polarimeter at the wavelength of sodium D band ( $\lambda = 589$  nm) using a quartz cuvette with a length of 10 cm ( $l = 1$  dm);  $^1\text{H-NMR}$  and  $^{13}\text{C-NMR}$  spectra were recorded on a Varian 500 spectrometer (scales settled on the solvents residual peaks: 7.26 ppm for  $\text{CDCl}_3$  and 3.31 ppm for  $\text{CD}_3\text{OD}$ ); Electrospray Ionization (ESI) mass spectrometry measurements (MS) were performed on a Esquire 4000 (Bruker–Daltonics) spectrometer; Infrared spectra (IR) were recorded on a Avatar 320-IR FT-IR (Thermo–Nicolet) spectrometer with a thin film of sample on NaCl crystal windows; Reverse Phase high-performance liquid chromatography (RP–HPLC) analyses were run on Amersham Pharmacia Biotech liquid chromatography equipped with UV Amersham detector, using a Gemini C18  $3 \mu\text{m} \times 150$  mm column for the analytical runs and a Gemini C18  $5 \mu\text{m} \times 250$  mm column for the semi-preparative ones.

### 2.3. Synthesis of 3,4-O-dicaffeoyl-1,5- $\gamma$ -quinide (6)

#### 2.3.1. 3,4-O-isopropyliden-1,5- $\gamma$ -quinide (11)

*D*-(–)-Quinic acid (3.0 g, 15.6 mmol) and *p*-toluenesulfonic acid (152 mg, 0.8 mmol) were suspended in distilled acetone (150 ml). The mixture was heated under reflux (56 °C) for 48 h in a Soxhlet apparatus, which was equipped with an extraction thimble filled with molecular sieves (4 Å, Merck), activated overnight in an oven at 120 °C. The reaction mixture was cooled to 0 °C using an ice-bath;  $\text{NaHCO}_3$  (364 mg, 10.3 mmol) was added and the suspension was stirred for 1 h. The mixture was filtered and the organic phase was evaporated under vacuum to obtain the product as a white solid (yield 93%). M.p. 133–136 °C;  $[\alpha]_{\text{D}}^{25} = -30.3$  ( $c = 1$ ,  $\text{CH}_3\text{OH}$ );  $^1\text{H NMR}$  (500 MHz,  $\text{CD}_3\text{OD}$ ):  $\delta$  1.32 (CCH<sub>3</sub>, s, 3H), 1.49 (CCH<sub>3</sub>, s, 3H), 2.02 (C<sub>2</sub>-H<sub>eq</sub>, dd, 1H,  $J_{\text{gem}} = 14.6$  Hz  $J_{\text{C}_2\text{Heq-C}_3\text{H}} = 3.0$  Hz), 2.26 (C<sub>6</sub>-H<sub>eq</sub>, dddd, 1H,  $J_{\text{gem}} = 11.7$  Hz  $J_{\text{C}_6\text{Heq-C}_5\text{H}} = 6.1$  Hz  $J_{\text{C}_6\text{Heq-C}_2\text{Hax}} = 2.3$  Hz  $J_{\text{C}_6\text{Heq-C}_4\text{H}} = 1.4$  Hz), 2.36 (C<sub>2</sub>-H<sub>ax</sub>, ddd, 1H,  $J_{\text{gem}} = 14.6$  Hz  $J_{\text{C}_2\text{Hax-C}_3\text{H}} = 7.7$  Hz  $J_{\text{C}_2\text{Hax-C}_6\text{Heq}} = 2.3$  Hz), 2.53 (C<sub>6</sub>-H<sub>ax</sub>, d, 1H,  $J_{\text{gem}} = 11.7$  Hz), 4.30 (C<sub>4</sub>-H, ddd, 1H,  $J_{\text{C}_4\text{H-C}_3\text{H}} = 6.5$  Hz  $J_{\text{C}_4\text{H-C}_5\text{H}} = 2.5$  Hz  $J_{\text{C}_4\text{H-C}_6\text{Heq}} = 1.4$  Hz), 4.52 (C<sub>3</sub>-H, ddd, 1H,  $J_{\text{C}_3\text{H-C}_2\text{Hax}} = 7.7$  Hz  $J_{\text{C}_3\text{H-C}_4\text{H}} = 6.5$  Hz  $J_{\text{C}_3\text{H-C}_2\text{Heq}} = 3.0$  Hz), 4.67 (C<sub>5</sub>-H, dd, 1H,  $J_{\text{C}_5\text{H-C}_6\text{Heq}} = 6.1$  Hz  $J_{\text{C}_5\text{H-C}_4\text{H}} = 2.5$  Hz);  $^{13}\text{C NMR}$  (125.4 MHz,  $\text{CD}_3\text{OD}$ ):  $\delta$  24.54 (q, CH<sub>3</sub>), 27.32 (q, CH<sub>3</sub>), 35.55 (t, C<sub>6</sub>), 38.98 (t, C<sub>2</sub>), 72.28 (d, C<sub>3</sub>), 72.90 (d, C<sub>4</sub>), 73.62 (s, C<sub>1</sub>), 76.62 (d, C<sub>5</sub>), 110.74 (s, C<sub>8</sub>), 180.03 (s, C<sub>7</sub>); IR (cm<sup>-1</sup>): 3583, 2932, 1777, 1315, 1161, 1075, 980; MS (ESI<sup>+</sup>): 215 *m/z* (50, [M–H]<sup>+</sup>), 237 *m/z* (100, [M–Na]<sup>+</sup>).

#### 2.3.2. 1-O-(2,2,2-trichloroethoxycarbonyl)-3,4-O-isopropyliden-1,5- $\gamma$ -quinide (12)

Compound **11** (592 mg, 2.77 mmol) and pyridine (0.55 ml, 6.80 mmol) were dissolved in  $\text{CH}_2\text{Cl}_2$  (6 ml). A solution of 2,2-trichloroethyl chloroformate (0.42 ml, 3.09 mmol) in  $\text{CH}_2\text{Cl}_2$  (2 ml) was added dropwise to the reaction mixture at 0 °C. The solution was stirred at 0 °C for 1 h and then at room temperature for 24 h. The mixture was sequentially washed with 1 M HCl (two times, 5 ml at a time) and with brine (two times, 8 ml at a time) and the organic layer was dried on anhydrous  $\text{Na}_2\text{SO}_4$ . The solvent was eliminated under reduced pressure to obtain an orange oil. The crude was dissolved in refluxing MeOH (6 ml) and cooled, the solution was stored overnight at 4 °C to precipitate **12** as a white powder (yield 57%). M.p. 153–156 °C;  $[\alpha]_{\text{D}}^{25} = -7.8$  ( $c = 1$ ,  $\text{CH}_2\text{Cl}_2$ );  $^1\text{H NMR}$  (500 MHz,  $\text{CDCl}_3$ ):  $\delta$  1.33 (CCH<sub>3</sub>, s, 3H), 1.52 (CCH<sub>3</sub>, s, 3H), 2.40 (C<sub>2</sub>-H<sub>eq</sub>, dd, 1H,  $J_{\text{gem}} = 14.7$  Hz  $J_{\text{C}_2\text{eq-C}_3\text{H}} = 2.4$  Hz), 2.56 (C<sub>2</sub>-H<sub>ax</sub>, ddd, 1H,  $J_{\text{gem}} = 14.7$  Hz,  $J_{\text{C}_2\text{Hax-C}_3\text{H}} = 7.7$  Hz,  $J_{\text{C}_2\text{Hax-C}_6\text{Heq}} = 2.3$  Hz), 2.65 (C<sub>6</sub>-H<sub>ax</sub>, d, 1H,  $J_{\text{gem}} = 11.4$  Hz), 3.06 (C<sub>6</sub>-H<sub>eq</sub>, dddd, 1H,  $J_{\text{gem}} = 11.4$  Hz  $J_{\text{C}_6\text{Heq-C}_5\text{H}} = 6.5$  Hz  $J_{\text{C}_6\text{Heq-C}_2\text{Hax}} = 2.3$  Hz  $J_{\text{C}_6\text{Heq-C}_4\text{H}} = 1.1$  Hz), 4.34 (C<sub>4</sub>-H, ddd, 1H,  $J_{\text{C}_4\text{H-C}_3\text{H}} = 5.3$  Hz  $J_{\text{C}_4\text{H-C}_5\text{H}} = 2.3$  Hz  $J_{\text{C}_4\text{H-C}_6\text{Heq}} = 1.1$  Hz), 4.55 (C<sub>3</sub>-H, ddd, 1H,  $J_{\text{C}_3\text{H-C}_2\text{Hax}} = 7.7$  Hz  $J_{\text{C}_3\text{H-C}_4\text{H}} = 5.3$  Hz  $J_{\text{C}_3\text{H-C}_2\text{Heq}} = 2.4$  Hz), 4.72 (C<sub>10</sub>-H, d, 1H,  $J_{\text{gem}} = 11.8$  Hz), 4.80 (C<sub>5</sub>-H, dd, 1H,  $J_{\text{C}_5\text{H-C}_6\text{Heq}} = 6.5$  Hz  $J_{\text{C}_5\text{H-C}_4\text{H}} = 2.3$  Hz), 4.82 (C<sub>10</sub>-H, d, 1H,  $J_{\text{gem}} = 11.8$  Hz);  $^{13}\text{C NMR}$  (125.4 MHz,  $\text{CDCl}_3$ ):  $\delta$  24.41 (q, CH<sub>3</sub>), 27.08 (q, CH<sub>3</sub>), 30.34 (t, C<sub>6</sub>), 35.42 (t, C<sub>2</sub>), 71.15 (d, C<sub>3</sub>), 72.46 (d, C<sub>4</sub>), 75.47 (d, C<sub>5</sub>), 77.09 (t, C<sub>10</sub>), 78.90 (s, C<sub>1</sub>), 94.03 (s, CCl<sub>3</sub>), 110.21 (s, C<sub>8</sub>), 151.50 (s, C<sub>9</sub>), 172.61 (s, C<sub>7</sub>); IR (cm<sup>-1</sup>) 2995, 2939, 1809, 1765, 1380, 1241, 1075, 736; MS (ESI<sup>+</sup>): 411 *m/z* (97, [M<sup>35</sup>Cl<sub>3</sub>–Na]<sup>+</sup>), 413 *m/z* (100, [M<sup>35</sup>Cl<sub>2</sub><sup>37</sup>Cl–Na]<sup>+</sup>), 415 *m/z* (25, [M<sup>35</sup>Cl<sup>37</sup>Cl<sub>2</sub>–Na]<sup>+</sup>).

#### 2.3.3. 1-O-(2,2,2-trichloroethoxycarbonyl)-1,5- $\gamma$ -quinide (13)

Trichloroacetic acid (373 mg, 2.28 mmol) was added to water (42  $\mu\text{l}$ ) and the mixture was heated until a clear solution was obtained. When the acidic aqueous solution reached room temperature, **12** (252 mg, 0.65 mmol) was added and reaction was stirred for 4 h. Ice-cooled water (5.7 ml), ethyl acetate (11.4 ml) and 40% aqueous  $\text{NaHCO}_3$  solution (11.4 ml) were added in order. The organic layer was separated from the aqueous one, that was further extracted with ethyl acetate (15 ml); the organic fractions were collected and washed with 2%  $\text{NaHCO}_3$  (15 ml) and water (12 ml). The organic phase was then dried over anhydrous  $\text{Na}_2\text{SO}_4$ , filtered and the solvent was removed under vacuum to obtain a powder. The residue was crystallized from toluene to afford the product as white crystals (yield 61%). M.p. 132–133 °C;  $[\alpha]_{\text{D}}^{25} = -4.6$  ( $c = 1$ ,  $\text{CH}_2\text{Cl}_2$ );  $^1\text{H NMR}$  (500 MHz,  $\text{CDCl}_3$ ):  $\delta$  1.67 (OH, br, 1H), 2.17 (C<sub>2</sub>-H<sub>ax</sub>, dd, 1H,  $J_{\text{gem}} = 11.6$  Hz  $J_{\text{C}_2\text{Hax-C}_3\text{H}} = 11.2$  Hz), 2.39 (C<sub>2</sub>-H<sub>eq</sub>, ddd, 1H,  $J_{\text{gem}} = 14.6$  Hz  $J_{\text{C}_2\text{Heq-C}_3\text{H}} = 6.7$  Hz  $J_{\text{C}_2\text{Heq-C}_6\text{Heq}} = 3.1$  Hz), 2.68 (C<sub>6</sub>-H<sub>ax</sub>, d, 1H,  $J_{\text{gem}} = 11.2$  Hz), 2.84 (OH, br, 1H), 3.06 (C<sub>6</sub>-H<sub>eq</sub>, ddd, 1H,  $J_{\text{gem}} = 11.2$  Hz  $J_{\text{C}_6\text{Heq-C}_5\text{H}} = 6.3$  Hz  $J_{\text{C}_6\text{Heq-C}_2\text{Heq}} = 3.1$  Hz), 4.03 (C<sub>3</sub>-H, ddd, 1H,  $J_{\text{C}_3\text{H-C}_2\text{Hax}} = 11.2$  Hz  $J_{\text{C}_3\text{H-C}_2\text{Heq}} = 6.7$  Hz  $J_{\text{C}_3\text{H-C}_4\text{H}} = 4.5$  Hz), 4.18 (C<sub>4</sub>-H, dd, 1H,  $J_{\text{C}_4\text{H-C}_3\text{H}} = 4.5$  Hz  $J_{\text{C}_4\text{H-C}_5\text{H}} = 4.5$  Hz), 4.74 (C<sub>9</sub>-H, d, 1H,  $J_{\text{gem}} = 11.8$  Hz), 4.81 (C<sub>9</sub>-H, d, 1H,  $J_{\text{gem}} = 11.8$  Hz), 4.93 (C<sub>5</sub>-H, ddd, 1H,  $J_{\text{C}_5\text{H-C}_6\text{Heq}} = 6.3$  Hz  $J_{\text{C}_5\text{H-C}_4\text{H}} = 4.5$  Hz);  $^{13}\text{C NMR}$  (125.4 MHz,  $\text{CDCl}_3$ ):  $\delta$  32.65 (t, C<sub>6</sub>), 36.53 (t, C<sub>2</sub>), 65.86 (d, C<sub>3</sub>), 65.95 (d, C<sub>4</sub>), 76.20 (d, C<sub>5</sub>), 77.11 (s, C<sub>1</sub>), 79.04 (t, C<sub>9</sub>), 94.03 (s, CCl<sub>3</sub>), 151.58 (s, C<sub>8</sub>), 171.44 (s, C<sub>7</sub>); IR (cm<sup>-1</sup>): 3412 (br), 1782, 1764, 1379, 1244, 1037, 665; MS (ESI<sup>-</sup>): 347 *m/z* (20, [M<sup>35</sup>Cl<sub>3</sub>–H]<sup>-</sup>), 349 *m/z* (20, [M<sup>35</sup>Cl<sub>2</sub><sup>37</sup>Cl–H]<sup>-</sup>), 351 *m/z* (5, [M<sup>35</sup>Cl<sup>37</sup>Cl<sub>2</sub>–H]<sup>-</sup>), 383 *m/z* (80, [M<sup>35</sup>Cl<sub>3</sub>–Cl]<sup>-</sup>), 385 *m/z* (100, [M<sup>35</sup>Cl<sub>2</sub><sup>37</sup>Cl–Cl]<sup>-</sup>), 386 *m/z* (50, [M<sup>35</sup>Cl<sup>37</sup>Cl<sub>2</sub>–Cl]<sup>-</sup>), 389 (20, [M<sup>37</sup>Cl<sub>3</sub>–Cl]<sup>-</sup>).

#### 2.3.4. 3,4-O-dimethoxycarbonyl caffeic acid (14)

Caffeic acid (2.01 g, 11 mmol) was dissolved in 1 M aqueous NaOH (40 ml) and cooled to 0 °C. Methyl chloroformate (2.04 ml, 26.4 mmol) was added dropwise and the mixture was stirred for

1 h at 0 °C and for 1 h at room temperature: in a few time a yellow powder began to precipitate. The reaction mixture was acidified with 2 M aqueous HCl to pH 1, the solid was collected by filtration and washed with water. Recrystallization from 50–50 v/v water–ethanol (28 ml) gave **14** as a yellow-earth powder (yield 90%). M.p.: 140–141 °C; <sup>1</sup>H NMR (500 MHz, CDCl<sub>3</sub>): δ 3.92 (OCH<sub>3</sub>, s, 3H), 3.93 (OCH<sub>3</sub>, s, 3H), 6.41 (C<sub>1</sub>-H, d, 1H, J = 15.9 Hz), 7.34 (C<sub>5</sub>-H, d, 1H, J<sub>ortho</sub> = 8.4 Hz), 7.46 (C<sub>4</sub>-H, dd, 1H, J<sub>ortho</sub> = 8.4 Hz, J<sub>meta</sub> = 1.9 Hz), 7.49 (C<sub>8</sub>-H, d, 1H, J<sub>meta</sub> = 1.9 Hz), 7.72 (C<sub>2</sub>-H, d, 1H, J = 15.9 Hz); <sup>13</sup>C NMR (125.4 MHz, CDCl<sub>3</sub>): δ 56.10 (q, 2C, OCH<sub>3</sub>), 118.92 (d, C<sub>1</sub>), 122.71 (d, C<sub>8</sub>), 123.72 (d, C<sub>5</sub>), 127.03 (d, C<sub>4</sub>), 133.26 (s, C<sub>3</sub>), 142.86 (s, C<sub>7</sub>), 144.07 (s, C<sub>6</sub>), 144.91 (d, C<sub>2</sub>), 153.03 (s, OCOO), 153.20 (s, OCOO), 171.58 (s, COOH); IR (cm<sup>-1</sup>): 2918.7, 1760.6, 1692.6, 1632.7, 1438.2, 1265.3, 932.1; MS (ESI<sup>-</sup>): 295 m/z (100, [M-H]<sup>-</sup>).

### 2.3.5. 3,4-dimethoxycarbonyl caffeic acid chloride (**15**)

A suspension of **14** (1.41 g, 4.76 mmol) in thionyl chloride (2.4 ml, 33 mmol, added dropwise) was heated to 90 °C until the formation of a homogeneous brown solution without gas development (~2 h). Before stopping the reaction, the mixture was checked by <sup>1</sup>H-NMR in CDCl<sub>3</sub> to control if the chlorination was finished. The unreacted thionyl chloride was removed under vacuum and the brown solid residue was recrystallized from toluene (10 ml) and filtered to obtain **15** as a yellow powder (yield 50%), that was used immediately after its preparation. <sup>1</sup>H NMR (500 MHz, CDCl<sub>3</sub>): δ 3.92 (OCH<sub>3</sub>, s, 3H), 3.93 (OCH<sub>3</sub>, s, 3H), 6.61 (C<sub>1</sub>-H, d, 1H, J = 15.6 Hz), 7.38 (C<sub>5</sub>-H, d, 1H, J<sub>ortho</sub> = 8.5 Hz), 7.48 (C<sub>4</sub>-H, dd, 1H, J<sub>ortho</sub> = 8.5 Hz, J<sub>meta</sub> = 2.1 Hz), 7.52 (C<sub>8</sub>-H, d, 1H, J<sub>meta</sub> = 2.1 Hz), 7.76 (C<sub>2</sub>-H, d, 1H, J = 15.6 Hz); <sup>13</sup>C NMR (125.4 MHz, CDCl<sub>3</sub>): δ 56.16 (q, 2C, OCH<sub>3</sub>), 123.36 (d, C<sub>8</sub>), 123.89 (d, C<sub>1</sub>), 123.97 (d, C<sub>5</sub>), 127.74 (d, C<sub>4</sub>), 132.05 (s, C<sub>3</sub>), 143.01 (s, C<sub>7</sub>), 144.96 (s, C<sub>6</sub>), 148.21 (d, C<sub>2</sub>), 152.81 (s, OCOO), 153.07 (s, OCOO), 165.88 (s, COCl); MS (ESI<sup>-</sup>): 334 m/z (100, [MOCH<sub>3</sub>-Na]<sup>+</sup>).

### 2.3.6. 1-O-(2,2,2-trichloroethoxycarbonyl)-3,4-bis[3,4-O-(dimethoxycarbonyl)caffeoyl]-1,5-γ-quinide (**16**)

Compound **13** (136 mg, 0.39 mmol) was dissolved in CH<sub>2</sub>Cl<sub>2</sub> (stored on CaCl<sub>2</sub>, 10 ml); DMAP (10 mg, 0.08 mmol) and Et<sub>3</sub>N (0.35 ml, 2.5 mmol) were added and the solution was cooled to 0 °C. Chloride **15** (600 mg, 1.9 mmol) was slowly added and the yellow solution was stirred for 1 h at 0 °C and then for 24 h at room temperature. The reaction mixture was sequentially washed with 1 M HCl (two times, 15 ml at a time), 2% NaHCO<sub>3</sub> (15 ml) and brine (10 ml); the organic layer was dried over Na<sub>2</sub>SO<sub>4</sub> and the solvent was removed by vacuum evaporation. The crude was purified by flash chromatography on silica gel (glass column 2.5 × 35 cm, gradient elution from CH<sub>2</sub>Cl<sub>2</sub>/ethyl acetate 98/2 to 92/8 v/v) to obtain **16** as a pearly powder (yield 40%). <sup>1</sup>H NMR (500 MHz, CDCl<sub>3</sub>): δ 2.46 (C<sub>2</sub>-H<sub>ax</sub>, dd, 1H, J<sub>gem</sub> = 11.8 Hz, J<sub>C2Hax-C3H</sub> = 11.6 Hz), 2.56 (C<sub>2</sub>-H<sub>eq</sub>, ddd, 1H, J<sub>gem</sub> = 11.8 Hz, J<sub>C2Heq-C3H</sub> = 6.8 Hz, J<sub>C2Heq-C6Heq</sub> = 2.7 Hz), 2.71 (C<sub>6</sub>-H<sub>ax</sub>, d, 1H, J<sub>gem</sub> = 11.6 Hz), 3.23 (C<sub>6</sub>-H<sub>eq</sub>, ddd, 1H, J<sub>gem</sub> = 11.6 Hz, J<sub>C6Heq-C5H</sub> = 5.9 Hz, J<sub>C6Heq-C2Heq</sub> = 2.7 Hz), 3.89 (OCH<sub>3</sub>, s, 3H), 3.90 (OCH<sub>3</sub>, s, 3H), 3.92 (OCH<sub>3</sub>, s, 3H), 3.93 (OCH<sub>3</sub>, s, 3H), 4.75 (C<sub>9</sub>-H, d, 1H, J<sub>gem</sub> = 11.8 Hz), 4.85 (C<sub>9</sub>-H, d, 1H, J<sub>gem</sub> = 11.8 Hz), 5.02 (C<sub>5</sub>-H, dd, 1H, J<sub>C5H-C6Heq</sub> = 5.9 Hz, J<sub>C5H-C4H</sub> = 4.9 Hz), 5.36 (C<sub>3</sub>-H, ddd, 1H, J<sub>C3H-C2Hax</sub> = 11.6 Hz, J<sub>C3H-C2Heq</sub> = 6.8 Hz, J<sub>C3H-C4H</sub> = 4.7 Hz), 5.71 (C<sub>4</sub>-H, dd, 1H, J<sub>C4H-C5H</sub> = 4.9 Hz, J<sub>C4H-C3H</sub> = 4.7 Hz), 6.28 (C<sub>11</sub>-H, d, 1H, J<sub>C11H-C12H</sub> = 16 Hz), 6.45 (C<sub>11</sub>-H, d, 1H, J<sub>C11H-C12H</sub> = 15.9 Hz), 7.27 (C<sub>15</sub>-H, d, 1H, J<sub>ortho</sub> = 8.5 Hz), 7.34 (C<sub>14</sub>-H and C<sub>15</sub>-H, m, 2H), 7.42 (C<sub>18</sub>-H and C<sub>14</sub>-H, m, 2H), 7.52 (C<sub>18</sub>-H, d, 1H, J<sub>meta</sub> = 1.9 Hz), 7.59 (C<sub>12</sub>-H, d, 1H, J<sub>C12H-C11H</sub> = 16 Hz), 7.67 (C<sub>12</sub>-H, d, 1H, J<sub>C12H-C11H</sub> = 15.9 Hz); <sup>13</sup>C NMR (125.4 MHz, CDCl<sub>3</sub>): δ 33.78 (t, C<sub>2</sub>), 33.87 (t, C<sub>6</sub>), 56.07 (q, 2C, 2OCH<sub>3</sub>), 56.11 (q, 2C, 2OCH<sub>3</sub>), 65.05 (d, C<sub>4</sub>), 66.12 (d, C<sub>3</sub>), 73.74 (d, C<sub>5</sub>), 78.78 (t, C<sub>9</sub>), 94.04 (s, CCl<sub>3</sub>),

114.2 (s, C<sub>1</sub>), 117.89 (d, C<sub>11</sub>), 118.11 (d, C<sub>11</sub>'), 122.45 (d, C<sub>18</sub>), 122.51 (d, C<sub>18</sub>'), 123.69 (d, C<sub>15</sub>), 123.81 (d, C<sub>15</sub>'), 127.05 (d, C<sub>14</sub>), 127.23 (d, C<sub>14</sub>'), 132.94 (s, C<sub>13</sub>), 133.16 (s, C<sub>13</sub>'), 142.83 (s, C<sub>17</sub>), 142.93 (s, C<sub>17</sub>'), 144.00 (s, C<sub>16</sub>), 144.21 (s, C<sub>16</sub>'), 144.35 (d, C<sub>12</sub>), 144.94 (d, C<sub>12</sub>'), 151.54 (s, C<sub>8</sub>), 152.97 (s, C<sub>19</sub>), 152.99 (s, C<sub>19</sub>'), 153.15 (s, C<sub>20</sub>), 153.21 (s, C<sub>20</sub>'), 164.61 (s, C<sub>10</sub>), 164.78 (s, C<sub>10</sub>'), 170.10 (s, C<sub>7</sub>); IR (cm<sup>-1</sup>): 3583.1, 2918.0, 1771.3, 1722.2, 1441.2, 1259.7, 1146.3, 727.9; MS (ESI<sup>+</sup>): 929.2 m/z (100, [M<sup>37</sup>Cl-Na]<sup>+</sup>).

### 2.3.7. 3,4-O-dicafeoyl-1,5-γ-quinide (**6**) (Blumberg, Frank, & Hofmann, 2010)

Compound **16** (438 mg, 0.48 mmol) was suspended in dry pyridine (stored on molecular sieves, 4.4 ml); LiCl (229 mg, 5.4 mmol) was added and then the mixture was stirred for 7 days at 50 °C. During the reaction time the suspension turned to a brown solution. The solvent was removed under vacuum and the residue was dissolved in ethyl acetate (20 ml), then sequentially washed with 2 M HCl (two times, 12 ml each one), 2% NaHCO<sub>3</sub> (two times, 10 ml each one) and brine (8 ml); the organic phase was dried on Na<sub>2</sub>SO<sub>4</sub> and the vacuum removal of the solvent gave an orange residue. The crude was treated by flash chromatography on polyamide MN-SC-6 (glass column 2 × 30 cm, gradient elution from ethyl acetate/methanol 80/20 to 50/50 v/v); the fractions rich in the target molecule were purified by semi-preparative RP-HPLC on a Phenomenex Gemini C18 5 μm 10 × 250 mm column (15 mg of crude for each run, loop 10 ml), using a gradient of H<sub>2</sub>O + 0.1% TFA (A) and MeOH + 0.1% TFA (B) (20 min A 80% B 20%, from 20 to 90 min increase of B until A 40% B 60%, from 90 to 110 min A 5% B 95%, from 110 to 125 min A 95% B 5%) at a flow rate of 2 ml/min. The elution was monitored with a UV/vis detector at λ 214, 288 and 325 nm; the fractions corresponding to the peak of interest were checked with ESI<sup>+</sup>-MS (molecular ion [M-H]<sup>+</sup> 499 m/z) and then freeze-dried: **6** was obtained as a white powder (yield 20%). M.p. 134–136 °C; <sup>1</sup>H NMR (500 MHz, CD<sub>3</sub>OD): δ 2.16 (C<sub>2</sub>-H<sub>ax</sub>, dd, 1H, J<sub>gem</sub> = 11.8 Hz, J<sub>C2Hax-C3H</sub> = 11.6 Hz), 2.28 (C<sub>2</sub>-H<sub>eq</sub>, ddd, 1H, J<sub>gem</sub> = 11.8 Hz, J<sub>C2Heq-C3H</sub> = 6.8 Hz, J<sub>C2Heq-C6Heq</sub> = 2.4 Hz), 2.47 (C<sub>6</sub>-H<sub>eq</sub>, ddd, 1H, J<sub>gem</sub> = 11.9 Hz, J<sub>C6Heq-C5H</sub> = 5.7 Hz, J<sub>C6Heq-C2Heq</sub> = 2.4 Hz), 2.59 (C<sub>6</sub>-H<sub>ax</sub>, d, 1H, J<sub>gem</sub> = 11.9 Hz), 4.92 (C<sub>5</sub>-H, dd, 1H, J<sub>C5H-C6Heq</sub> = 5.7 Hz, J<sub>C5H-C4H</sub> = 5.1 Hz), 5.18 (C<sub>3</sub>-H, ddd, 1H, J<sub>C3H-C2Hax</sub> = 11.6 Hz, J<sub>C3H-C2Heq</sub> = 6.8 Hz, J<sub>C3H-C4H</sub> = 4.7 Hz), 5.61 (C<sub>4</sub>-H, dd, 1H, J<sub>C4H-C5H</sub> = 5.1 Hz, J<sub>C4H-C3H</sub> = 4.7 Hz), 6.14 (C<sub>9</sub>-H, d, 1H, J<sub>C9H-C10H</sub> = 15.9 Hz), 6.37 (C<sub>9</sub>-H, d, 1H, J<sub>C9H-C10H</sub> = 15.8 Hz), 6.68 (C<sub>13</sub>-H, d, 1H, J<sub>ortho</sub> = 8.2 Hz), 6.80 (C<sub>12</sub>-H and C<sub>13</sub>-H, m, 2H), 6.98 (C<sub>16</sub>-H and C<sub>12</sub>-H, m, 2H), 7.08 (C<sub>16</sub>-H, d, 1H, J<sub>meta</sub> = 2.0 Hz), 7.48 (C<sub>10</sub>-H, d, 1H, J<sub>C10H-C9H</sub> = 15.9 Hz), 7.63 (C<sub>10</sub>-H, d, 1H, J<sub>C10H-C9H</sub> = 15.8 Hz); <sup>13</sup>C NMR (125.4 MHz, CD<sub>3</sub>OD): δ 37.36 (t, C<sub>2</sub>), 38.70 (t, C<sub>6</sub>), 65.89 (d, C<sub>4</sub>), 67.79 (d, C<sub>3</sub>), 72.89 (s, C<sub>1</sub>), 75.07 (d, C<sub>5</sub>), 113.95 (d, C<sub>9</sub>), 114.07 (d, C<sub>9</sub>'), 114.81 (d, C<sub>16</sub>), 115.34 (d, C<sub>16</sub>'), 116.42 (d, C<sub>13</sub>), 116.55 (d, C<sub>13</sub>'), 123.41 (d, C<sub>12</sub>), 123.49 (d, C<sub>12</sub>'), 127.45 (s, C<sub>11</sub>), 127.50 (s, C<sub>11</sub>'), 146.81 (s, C<sub>15</sub>), 146.89 (s, C<sub>15</sub>'), 147.87 (d, C<sub>10</sub>), 148.55 (d, C<sub>10</sub>'), 149.81 (s, C<sub>14</sub>), 150.00 (s, C<sub>14</sub>'), 167.37 (s, C<sub>8</sub>), 167.54 (s, C<sub>8</sub>'), 178.22 (s, C<sub>7</sub>); IR (cm<sup>-1</sup>): 3405.7, 2950.7, 1790.6, 1633.0, 1269.35, 1020.7, 644.9; MS (ESI<sup>+</sup>): 499 m/z (100, [M-H]<sup>+</sup>).

### 2.4. Fluorescence spectroscopy

Compounds **2**, **3**, **5**, **6**, **7**, **8**, **9**, and **10** stock solutions (7 mM, 1.4 mM, 350 μM and for **6** 87.5 μM) were prepared in DMSO.

Steady state fluorescence spectra were recorded at 25 °C on a CARY Eclipse (Varian) spectrofluorimeter equipped with a 1 cm quartz cuvette (λ<sub>exc</sub> 280 nm, λ<sub>em</sub> 340 nm). The emission corresponding to λ<sub>exc</sub> 280 nm was recorded in the λ<sub>em</sub> range 300–400 nm. Synchronous fluorescence spectra (SFS) were measured by setting the excitation wavelength in the 240–320 nm

range, and the emission was recorded at  $\Delta = 60$  nm in the 300–380 nm range. The slit width on the excitation was set to 10 nm, on the emission to 20 nm. The concentration of HSA essentially fatty acid free solutions was 0.5  $\mu$ M in 350  $\mu$ l of solvent (135  $\mu$ l of phosphate buffer 10 mM in  $\text{Na}_2\text{HPO}_4$  and 2 mM in  $\text{KH}_2\text{PO}_4$  diluted in 215  $\mu$ l of mQ water, pH 7.4) for all the measurements; the ligand concentration was gradually increased during the titration from 1  $\mu$ M to 500  $\mu$ M by adding aliquots of their stock solutions; the final amount of DMSO was always less than 8%, and it has been verified that such amounts of the solvent do not affect the fluorescence of HSA. For compound **6** the fluorescence quenching with a titration in a narrower concentration range (from 0.25 to 200  $\mu$ M) was also measured. After each addition of the ligand, the emission spectra, the fluorescence intensity, and the SFS were recorded. All the analyses were replicated three times.

The displacement of warfarin was studied with the same spectrofluorimeter and cell, in the same buffer described above for the binding study. Warfarin was added to the buffer at a 10 mM final

concentration from a 1 mM reference solution in DMSO. HSA was then added at a 2.5 mM final concentration from a 250 mM reference solution in water, and the emission spectrum was recorded upon excitation of bound warfarin at 320 nm. The emission maximum was observed at 380 nm. Lactone **6** was then added at increasing concentrations by adding aliquots of its stock solution in the 400 nM–72 mM range, and the emission spectrum was recorded again at each addition.

### 3. Results and discussion

#### 3.1. Synthesis of the quinide ligands

Quinide **6** has been synthesized as reported in Fig. 2, by revising and improving a methodology reported by Blumberg (Blumberg et al., 2010). Unfortunately, using the procedure reported in the literature, we always afforded a mixture of monoesters on carbons 3 or 4 of the quinide and only a small amount of the diester was

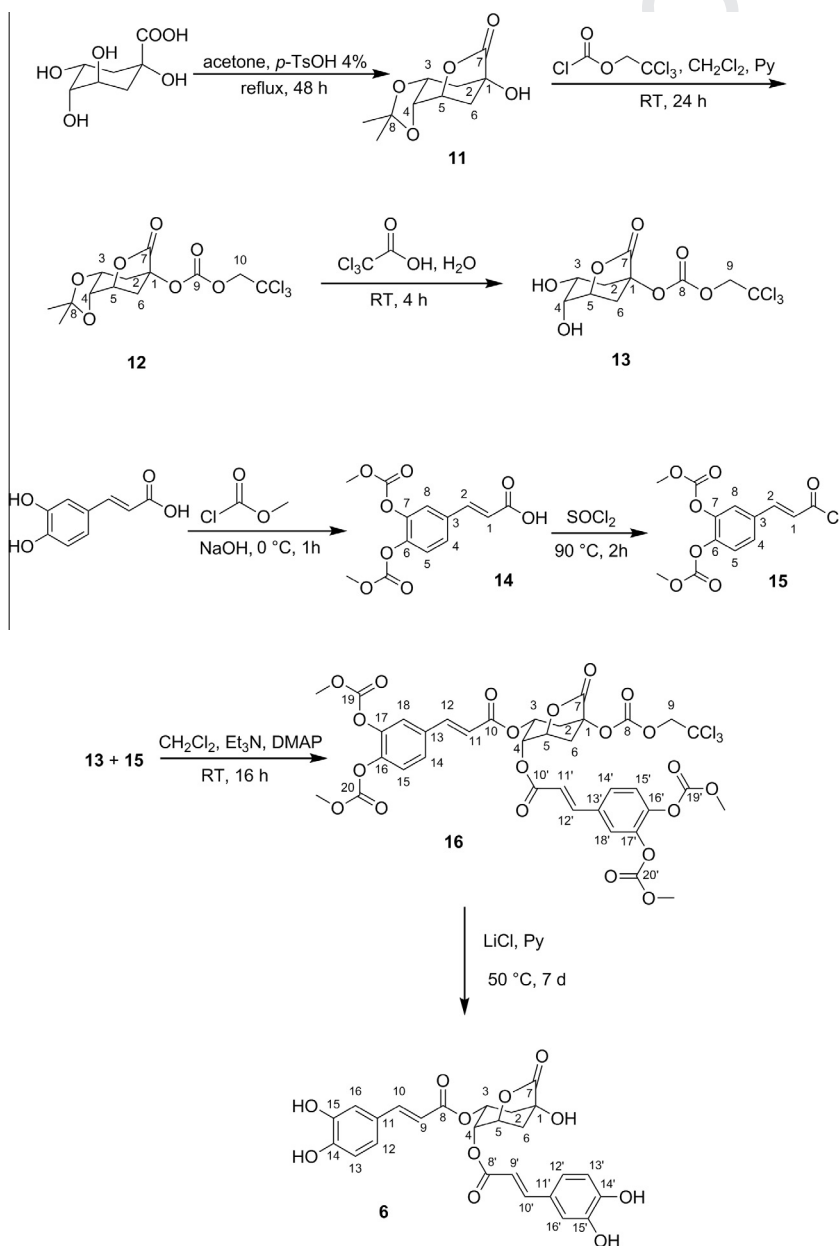


Fig. 2. Synthesis of compound **6**.

419 achieved. It was necessary to modify it in some steps to obtain the  
420 diester as the only coupling product: we have verified that it is of  
421 the utmost importance to have the intermediates **13** and **15** in the  
422 highest purity state before carrying out their coupling, and that the  
423 maximum yield is obtained using Et<sub>3</sub>N and DMAP as base instead  
424 of pyridine. All the intermediates were isolated as pure compounds  
425 and completely characterized by NMR spectroscopy.

426 The synthesis of quinides **7**, **8** and **9** have been described in  
427 details in our previous work (Sinisi et al., 2013).

### 428 3.2. HSA fluorescence and quenching

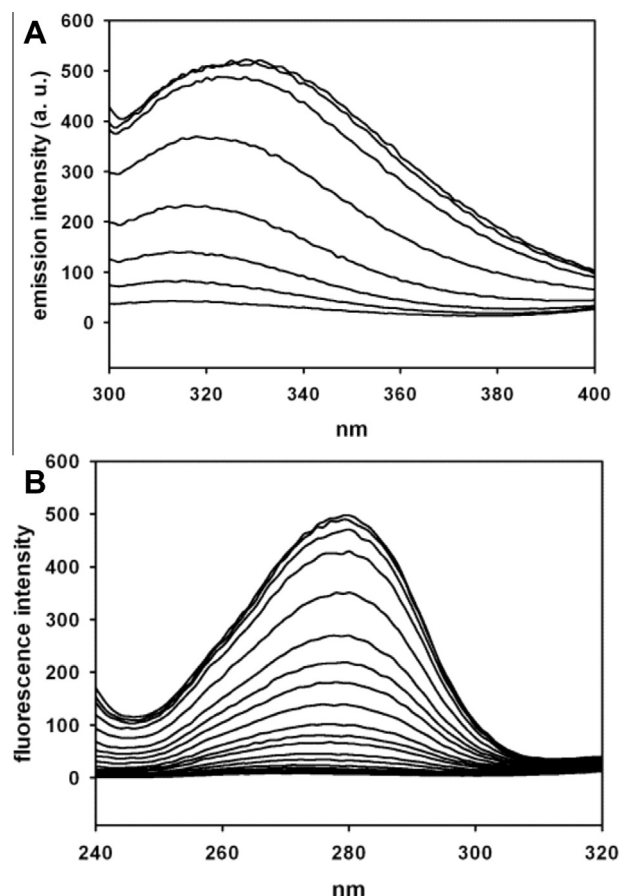
429 The interactions of the eight ligands with essentially fatty acid  
430 free HSA were studied monitoring the tryptophan-214 fluores-  
431 cence intensity: the excitation and emission wavelengths were  
432 set to 280 and 340 nm respectively, corresponding to the excita-  
433 tion and emission maxima of the protein measured in the absence  
434 of ligands. Emission spectra in the range 300–400 nm were also  
435 recorded to monitor the eventual environmental changes near the  
436 fluorophore by shifts in the emission maximum wavelength,  
437 while synchronous spectra with a wavelength shift of 60 nm  
438 also recorded to distinguish between the tryptophan and the  
439 tyrosine residues (Dockal, Carter, & Rüker, 2000). Fluorescence  
440 quenching titrations were carried out by increasing the ligand  
441 concentration while keeping the concentration of protein constant.  
442 Under these conditions only 3,4-*O*-dimethoxy cinnamic acid **10**  
443 showed interferences due to its intrinsic fluorescence emission,  
444 which is greater at lower concentrations (such self-quenching is  
445 most likely due to aggregation at higher concentrations). To avoid  
446 this interference we subtracted the blank fluorescence of this  
447 ligand from the experimental data. We have also verified that sim-  
448 ilar corrections were not necessary in all the other measurements.

449 HSA fluorescence quenching was observed with all the tested  
450 ligands in the same experimental conditions; in Fig. 3 the emission  
451 spectra (A) and the synchronous spectra (B) of HSA for compound  
452 **5**, taken as an example, are reported. Fig. 3A shows how the emis-  
453 sion of the Trp residue, excited at 280 nm, changes during the titra-  
454 tion (the fluorescence quenching full data for each ligand are  
455 reported in the Supplementary data): the emission intensity  
456 decreases while the emission maximum evidently moves to lower  
457 wavelengths and the observed blue shifts are at least of 10 nm; this  
458 shift is consistent with a change of the environmental polarity  
459 surrounding the Trp residue, resulting from replacement of the sol-  
460 vent in the active site by the less polar molecules of ligand (Liu,  
461 Zheng, Yang, Wang, & Wang, 2009). The use of DMSO for the  
462 ligands solutions does not contribute to the blue shift, as we have  
463 verified by adding only DMSO in the same experimental conditions  
464 of all the titrations.

465 A further confirmation of this microenvironmental modification  
466 near the fluorophore is given by the effects of the ligand addition  
467 on the synchronous emission spectra, as that shown in Fig. 3B,  
468 with a slight blue shift similar in all the ligands (on average the max-  
469 imum shifts from 280 to 278 nm). In both the emission and syn-  
470 chronous spectra the fluorescence intensity decreases down to  
471 zero with increasing ligand concentration and the amount of  
472 quenching measured in the synchronous experiments replicates  
473 those obtained in the corresponding fluorescence titration, sug-  
474 gesting that the quenching phenomenon is related to tryptophan  
475 emission.

476 To determine whether the observed quenching was due to  
477 binding or collisional phenomena, the emission data were analysed  
478 according to the Stern–Volmer equation (Eq. (1)):

$$481 \frac{F_0}{F} = 1 + K_q \tau_0 [Q] = 1 + K_{SV} [Q] \quad (1)$$



482 Fig. 3. (A) Emission spectra of HSA ( $\lambda_{\text{ex}} = 280 \text{ nm}$ ) in the presence of compound **5**;  
483 the concentrations of the ligands increase from top to bottom (0, 1, 5, 20, 60, 120,  
484 180, 250  $\mu\text{M}$ ), while the protein concentration is fixed to 0.5  $\mu\text{M}$ . (B) Synchronous  
485 spectra of HSA fluorescence emission in the presence of compound **5**; the  
486 concentrations of the ligands increase from top to bottom (0, 1, 5, 10, 20, 40, 60,  
487 80, 100, 120, 140, 160, 180, 200, 250, 300, 350, 400, 450, 500  $\mu\text{M}$ ), while the protein  
488 concentration in a and b is fixed to 0.5  $\mu\text{M}$ .

489 In Eq. (1)  $F_0$  and  $F$  are the emission intensities before and after the  
490 addition of the quencher, respectively,  $K_q$  is the bimolecular  
491 quenching kinetic constant,  $\tau_0$  is the lifetime of the fluorophore  
492 (for the tryptophan fluorescence decay  $\tau_0$  is about  $10^{-8} \text{ s}$ )  
493 (Kragh-Hansen, 1990),  $K_{SV}$  is the Stern–Volmer quenching constant  
494 and  $[Q]$  is the quencher concentration in mol/l; the protein concen-  
495 tration was fixed to 0.5  $\mu\text{M}$ . The  $K_{SV}$  for all the ligands were deter-  
496 mined by linear regression of a plot of  $F_0/F$  against  $[Q]$  (Fig. 4) in the  
497 ligand concentration range 0–140  $\mu\text{M}$ , where all the plots were linear:  
498 high concentrations of molecule indeed cause a deviation from  
499 the linearity more or less evident in the different cases, probably  
500 because large amounts of ligand in solution complicate the quench-  
501 ing mechanism (Min et al., 2004), with the progressive increase of  
502 the dynamic quenching contribution;  $K_{SV}$  and  $K_q$  (calculated using  
503 the equivalence  $K_q = K_{SV}/\tau_0$ ) are reported in Table 1, together with  
504 the binding parameters which will be discussed in the next section.

### 505 3.3. Dissociation constants and binding sites

506 The number of binding sites and the ligand–protein dissociation  
507 constants were extrapolated from the fluorescence data by a Hill  
508 analysis (Goutelle et al., 2008), using Eq. (2):

$$509 \log \left( \frac{Y}{1-Y} \right) = n \log [Q] - \log K_D \quad (2)$$

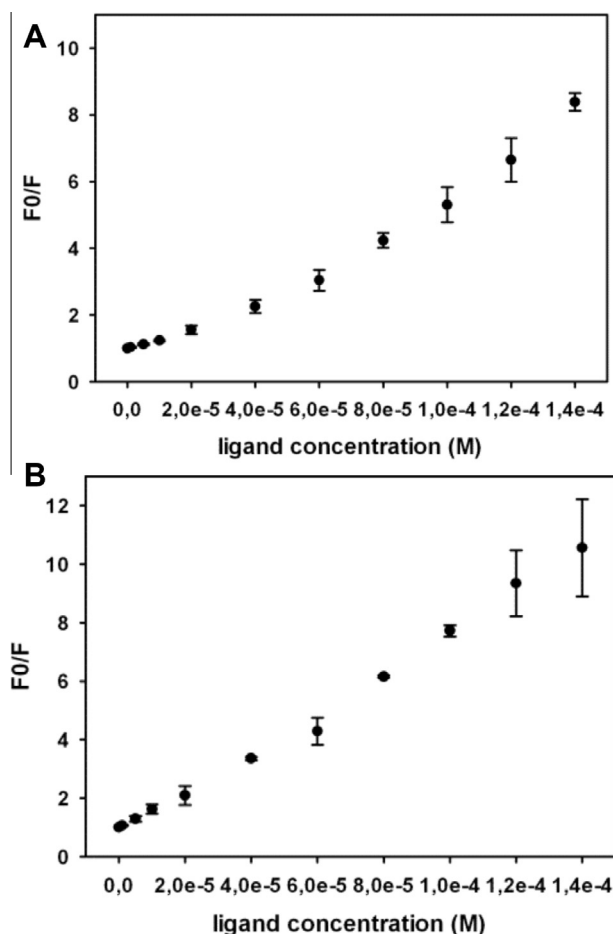


**Fig. 4.** Stern–Volmer plots of fluorescence quenching of HSA ( $\lambda_{\text{ex}} = 280$  nm,  $\lambda_{\text{em}} = 340$  nm) in the presence of compounds **3** (A), **9** (B), and **10** (C).

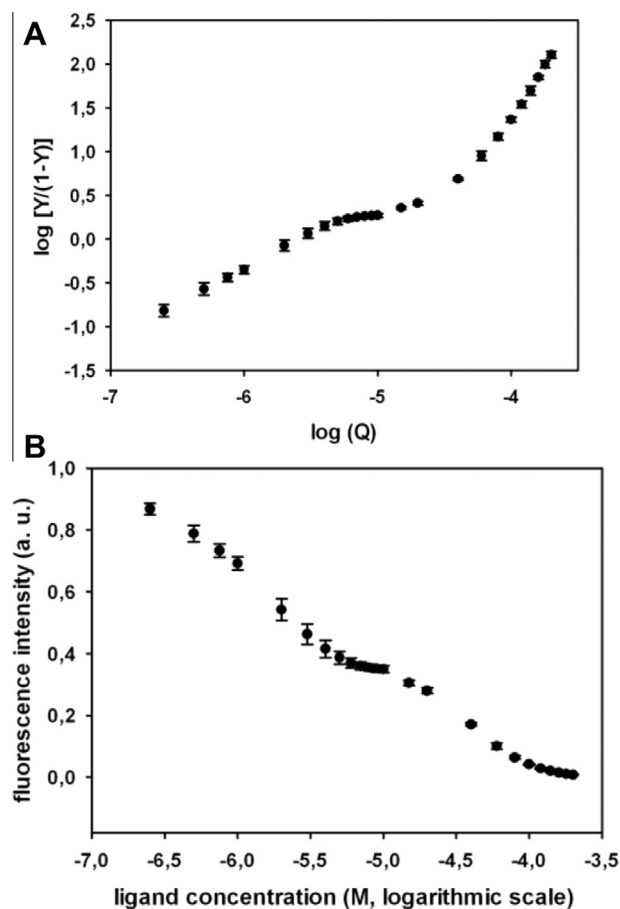


**Fig. 5.** Effect of the addition of compound **6** on the fluorescence intensity (the protein concentration is fixed to  $0.5 \mu\text{M}$ , while the ligand concentration range is  $0\text{--}200 \mu\text{M}$ ) (A) and the related Hill plot (B).

where  $Y$  is the fraction of free binding sites (calculated as  $1 - F/F_0$ , assuming that the ratio  $F/F_0$  gives the fraction of occupied binding sites),  $[Q]$  is the quencher concentration in mol/l,  $n$  is the number of binding sites, so it gives the stoichiometry of the interaction, and  $K_D$  is the dissociation constant.

All the ligands show linear Hill plots in the concentration range  $0\text{--}140 \mu\text{M}$ , with the exception of lactone **6**. The parameters  $n$  and  $-\log K_D$  for all the other ligands (Table 1) were obtained by linear regression of the Hill plot.

Compound **6** halves the fluorescence intensity even at concentrations as low as  $1 \mu\text{M}$ , and to understand more about this case we decided to investigate better the interaction in the ligand concentration range  $0\text{--}200 \mu\text{M}$ , keeping the protein concentration fixed to  $0.5 \mu\text{M}$ . A double, consecutive sigmoidal behaviour can be clearly seen (Fig. 5A), while in the Hill plot the slope suddenly

shifts from 1 to 2 (Fig. 5B). This may be due to the binding of two molecules of **6** inside the same albumin binding site. Such an unusual event in protein–ligand interaction has been recently reported for albumin, in the simultaneous binding of different drug molecules at this binding site (Yang et al., 2012).

We have evaluated the two binding constants (Table 1) by regression of the experimental data to Eq. (3) (see the Supplementary data for its derivation):

$$\frac{\Delta F}{F_0} = x \frac{\frac{[L]}{K_1}}{1 + \frac{[L]}{K_1}} + (1 - x) \frac{\frac{[L]^2}{K_1 K_2}}{1 + \frac{[L]}{K_1} + \frac{[L]^2}{K_1 K_2}} \quad (3)$$

where  $\Delta F$  is calculated as  $(F_0 - F)$ ,  $F_0$  and  $F$  are the fluorescence intensities before and after the addition of the quencher, respectively,  $[L]$  is the quencher concentration in mol/l,  $K_1$  is the dissociation constant for the protein–ligand complex with stoichiometry

**Table 1**

Quenching constants according to Stern–Volmer analysis: Stern–Volmer quenching constant ( $K_{\text{SV}}$ ) and bimolecular quenching kinetic constant ( $K_q$ ).

Ligand	Quenching constants			Binding parameters		
	$K_{\text{SV}} \pm \text{SD}$ ( $10^4 \text{ L mol}^{-1}$ )	$K_q \pm \text{SD}$ ( $10^{12} \text{ L mol}^{-1} \text{ s}^{-1}$ )	$R$	$n \pm \text{SD}$	$K_D \pm \text{SD}$ ( $\mu\text{mol L}^{-1}$ )	$R$
Acid <b>2</b>	$8.57 \pm 0.50$	$8.57 \pm 0.50$	0.98	$1.20 \pm 0.03$	$2.32 \pm 0.06$	0.99
Acid <b>3</b>	$4.96 \pm 0.26$	$4.96 \pm 0.26$	0.99	$1.04 \pm 0.04$	$21.2 \pm 0.8$	0.99
Acid <b>5</b>	$5.29 \pm 0.47$	$5.29 \pm 0.47$	0.97	$1.12 \pm 0.06$	$9.15 \pm 0.48$	0.99
Acid <b>10</b>	$4.23 \pm 0.17$	$4.23 \pm 0.17$	0.99	$0.99 \pm 0.03$	$31.1 \pm 1.1$	0.99
Lactone <b>6</b>	$43.84 \pm 4.12$	$43.84 \pm 4.12$	0.96	/	$K_1$ 0.967 $K_2$ 20.8	
Lactone <b>7</b>	$13.75 \pm 1.11$	$13.75 \pm 1.11$	0.97	$1.08 \pm 0.06$	$12.1 \pm 0.8$	0.96
Lactone <b>8</b>	$9.81 \pm 0.18$	$9.81 \pm 0.18$	0.99	$1.08 \pm 0.02$	$4.31 \pm 0.06$	0.99
Lactone <b>9</b>	$6.86 \pm 0.17$	$6.86 \pm 0.17$	0.99	$1.02 \pm 0.02$	$13.3 \pm 0.2$	0.99

535 1:1,  $K_2$  the dissociation constant for that with stoichiometry 1:2,  $x$  is  
536 a coefficient that allows to take into account the different quench-  
537 ing efficiency in the two possible complexes.

538 All the tested ligands cause the HSA fluorescence quenching and  
539 both the emission and the synchronous spectra suggest that the  
540 molecules enter in the subdomain IIA and interact with Trp-214.  
541 The bimolecular quenching kinetic constants ( $K_q$ ), showed in  
542 Table 1, are at least 3–4 orders of magnitude higher than the higher  
543 value for diffusion limited collisional quenching ( $2.0 \times 10^{10} -$   
544  $L \text{ mol}^{-1} \text{ s}^{-1}$ ) (Eftink, 1991), thus the static quenching originating  
545 from the association of the fluorophore and quenchers in a bimo-  
546 lecular complex is the main contribution to the fluorescence  
547 quenching mechanism within the 0–140  $\mu\text{M}$  ligand concentration  
548 range. Higher ligand concentrations complicate the quenching  
549 mechanism because the dynamic collision contribution becomes  
550 more significant.

551 Having thus established that the quenching data can be safely  
552 used for measuring the binding parameters, we can evaluate the  
553 results of the Hill analysis, showed in Table 1. The slope ( $n$ ) in  
554 the Hill plots is near 1 for all the ligands with the exception of com-  
555 pound 6, which means a 1:1 interaction stoichiometry between  
556 ligand and protein. In the case of compound 6, the trend of the  
557 fluorescence emission intensity during the titration and the sudden  
558 slope shift from 1 to 2 in the Hill plot suggest a 1:1 stoichiometry at  
559 low ligand concentration, switching to a 1:2 ratio at higher concen-  
560 trations, revealing the binding of two molecules of 6 inside the  
561 same albumin binding site, as both the molecules of 6 must be in  
562 proximity of Trp 214 in order to obtain fluorescence quenching  
563 upon binding. All the calculated  $K_D$  are in the micromolar range,  
564 showing a remarkably high affinity of these molecules for the pro-  
565 tein. The binding constants of 2, 3 and 5 (2.3, 21.2 and 9.2  $\mu\text{M}$   
566 respectively) are comparable in magnitude and trend to the  
567 published ones (6, 40 and 25  $\mu\text{M}$ ) (Hu et al., 2012; Kang et al.,  
568 2004; Min et al., 2004); among the carboxylic acids, compound  
569 10 shows the lowest affinity, probably due to the replacement of  
570 both phenolic hydroxyl groups with methoxyl ones: this leaves  
571 only the acid moiety capable to form hydrogen bonds, that can  
572 strengthen the ligand–protein interaction (Bartolomè, Estrella, &  
573 Hernández, 2000), with the polypeptide chain within the binding  
574 site. For lactones 7, 8 and 9, the second has a better affinity and this  
575 may be explained as a consequence of the free hydroxyl group in  
576 position 1 on the quinide core and of the presence of two aromatic  
577 rings instead of one as in lactone 7, enhancing the ability to estab-  
578 lish hydrophobic interactions, and of its lower dimension com-  
579 pared to lactone 9, that makes easier the entrance of the  
580 molecule in the active site.

581 We want to highlight the very interesting case of lactone 6: HSA  
582 seems capable to host two molecules of it in the same binding site,  
583 and the  $K_1$  is even in the hundred nanomolar range. To our knowl-  
584 edge, this is the lowest affinity ever reported for albumin, and by  
585 far more favourable than binding of most drugs to this protein.  
586 We have evaluated also the ability of lactone 6 to displace a drug  
587 from the binding site of albumin. We have chosen warfarin as this  
588 drug is the reference ligand of Sudlow site I; moreover, the intrinsic  
589 fluorescence of warfarin is strongly enhanced by the interactions  
590 with albumin, and decreases upon competition with other drugs  
591 for the protein. This phenomenon has been exploited to set up a  
592 well established method to study drug association to HSA  
593 (Sudlow, Birkett, & Wade, 1975b). The experiment was carried on  
594 a 10  $\mu\text{M}$  solution of warfarin in phosphate buffer, containing  
595 2.5  $\mu\text{M}$  HSA. By adding increasing concentrations of lactone 6,  
596 the displacement of warfarin from the albumin binding site can  
597 be clearly seen from the decrease of its fluorescence emission  
598 (Fig. 6). 50% of the initially bound drug is displaced at a 12  $\mu\text{M}$   
599 concentration of lactone 6, while warfarin is fully squeezed out at  
600 70  $\mu\text{M}$  lactone. Data regression to a hyperbolic binding isothermal

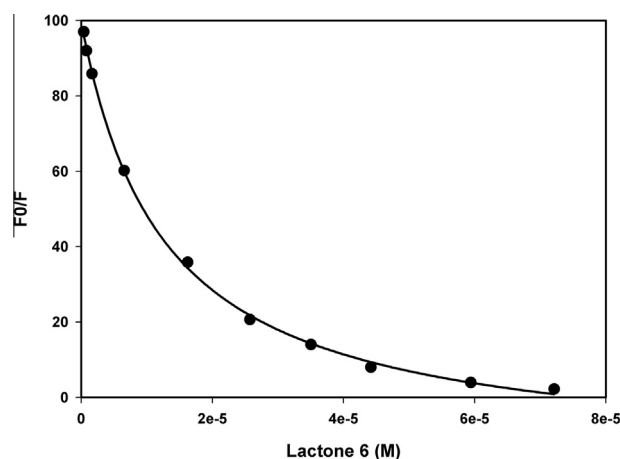


Fig. 6. Displacement of warfarin by compound 6: the fluorescence emission of HSA-bound warfarin (excitation 320 nm/emission 380 nm) was measured on a 10  $\mu\text{M}$  warfarin, 2.5  $\mu\text{M}$  HSA solution. The emission decays upon addition of the 400 nM–72  $\mu\text{M}$  range.

601 gives an apparent dissociation constant for lactone 6 of 12.4  $\mu\text{M}$  at  
602 10  $\mu\text{M}$  warfarin.

#### 603 4. Conclusions

604 In summary, we have demonstrated that HSA is able to bind all  
605 the considered ligands, with the formation of a bimolecular com-  
606 plex within the Sudlow site I. The dissociation constants show a  
607 very high affinity of the protein towards this family of compounds,  
608 moreover minimal changes in the chemical structure lead to signif-  
609 icant changes in binding. A reference drug warfarin is fully  
610 displaced from albumin by low concentrations of lactone 6; this  
611 result suggest that the dietary assumption of polyphenols from  
612 coffee and other sources could affect the pharmacokinetic profile  
613 of drugs binding to serum albumin.

#### 614 Acknowledgments

615 We thank Dr. Filomena Guida and Professor Alessandro Tossi  
616 (Department of Life Science, University of Trieste, Italy) for the pos-  
617 sibility to use their HPLC and for their precious help during the  
618 analysis. The University of Trieste is gratefully acknowledged for  
619 financial support.

#### 620 Appendix A. Supplementary data

621 Supplementary data associated with this article can be found, in  
622 the online version, at <http://dx.doi.org/10.1016/j.foodchem.2014.07.080>.  
623

#### 624 References

- 625 Anna, S. (2002). Interaction of drugs with bovine and human serum albumin. *Journal*  
626 *of Molecular Structure*, 614, 227–232.  
627 Bartolomè, B., Estrella, I., & Hernández, M. T. (2000). Interaction of low molecular  
628 weight phenolics with proteins (BSA). *Journal of Food Science*, 65, 617–621.  
629 Blumberg, S., Frank, O., & Hofmann, T. (2010). Quantitative studies on the influence  
630 of the bean roasting parameters and hot water percolation on the  
631 concentrations of bitter compounds in coffee brew. *Journal of Agricultural and*  
632 *Food Chemistry*, 58, 3720–3728.  
633 Clifford, M. N. (1985). Chlorogenic acids. In R. J. Clarke & R. Macrae (Eds.), *Coffee,*  
634 *Vol. 1, Chemistry* (pp. 153–202). London: Elsevier Applied Science Publ..  
635 Clifford, M. N. (2000). Chlorogenic acids and other cinnamates: Nature, occurrence,  
636 dietary burden, absorption, and metabolism. *Journal of the Science of Food and*  
637 *Agriculture*, 80, 1033–1043.

- 638 Clifford, M. N., Knight, S., Surucu, B., & Kuhnert, N. (2006). Characterization by LC-  
639 MS<sup>n</sup> of four new classes of chologenic acids in green coffee beans:  
640 Dimethoxycinnamoylquinic acids, diferuloylquinic acids, caffeoyl-  
641 dimethoxycinnamoylquinic acids, and feruloyl-dimethoxycinnamoylquinic  
642 acids. *Journal of Agricultural and Food Chemistry*, *54*, 1957–1969.
- 643 de Paulis, T., Schmidt, D. E., Bruchey, A. K., Kirby, M. T., McDonald, M. P.,  
644 Commers, P., et al. (2002). Dicinnamoylquinides in roasted coffee inhibit the  
645 human adenosine transporter. *European Journal of Pharmacology*, *442*,  
646 215–223.
- 647 Dockal, M., Carter, D. C., & Rüker, F. (2000). Conformational transitions of the three  
648 recombinant domains of human serum albumin depending on pH. *Journal of*  
649 *Biological Chemistry*, *275*, 3042–3050.
- 650 Eftink, M. R. (1991). Fluorescence quenching reactions: Probing biological macro-  
651 molecular structures. In T. G. Dewey (Ed.), *Biophysical and biochemical aspects of*  
652 *fluorescence spectroscopy* (pp. 105–133). New York: Plenum.
- 653 Farah, A., de Paulis, T., Trugo, L. C., & Martin, P. R. (2005). Effect of roasting on the  
654 formation of chlorogenic acid lactones in coffee. *Journal of Agricultural and Food*  
655 *Chemistry*, *53*, 1505–1513.
- 656 Farah, A., Monteiro, M., Donangelo, C. M., & Lafay, S. (2008). Chlorogenic acids from  
657 green coffee extract are highly bioavailable in humans. *Journal of Nutrition*, *138*,  
658 2309–2315.
- 659 Farrell, T. L., Gomez-Juaristi, M., Poquet, L., Redeuil, K., Nagy, K., Renouf, M., et al.  
660 (2012). Absorption of dimethoxycinnamic acid derivatives in vitro and  
661 pharmacokinetic profile in human plasma following coffee consumption.  
662 *Molecular Nutrition & Food Research*, *56*, 1413–1423.
- 663 Gloess, A. N., Schönbacher, B., Klopprogge, B., D'Ambrosio, L., Chatelain, K.,  
664 Bongartz, A., et al. (2013). Comparison of nine common coffee extraction  
665 methods: Instrumental and sensory analysis. *European Food Research and*  
666 *Technology*, *236*, 607–627.
- 667 Ghuman, J., Zunsain, P. A., Petipas, I., Bhattacharya, A. A., Otagiri, M., & Curry, S.  
668 (2005). Structural basis of the drug-binding specificity of human serum  
669 albumin. *Journal of Molecular Biology*, *353*, 38–52.
- 670 Goutelle, S., Maurin, M., Rougier, F., Barbaut, X., Bourguignon, L., Ducher, M., et al.  
671 (2008). The Hill equation: a review of its capabilities in pharmacological  
672 modeling. *Fundamental & Clinical Pharmacology*, *22*, 633–648.
- 673 He, X. M., & Carter, D. C. (1992). Atomic structure and chemistry of human serum  
674 albumin. *Nature*, *358*, 209–215.
- 675 Hu, Y. J., Chen, C. H., Zhou, S., Bai, A. M., & Ou-Yang, Y. (2012). The specific binding of  
676 chlorogenic acid to human serum albumin. *Molecular Biology Reports*, *39*,  
677 2781–2787.
- 678 IUPAC Commission on the Nomenclature of Organic Chemistry (CNOC) and IUPAC-  
679 IUB Commission on Biochemical Nomenclature (CBN), (1976). *Biochemical*  
680 *Journal*, *153*, 23–31.
- 681 Kang, J., Yuan, L., Meng-Xia, X., Song, L., Min, J., & Ying-Dian, W. (2004). Interactions  
682 of human serum albumin with chlorogenic acid and ferulic acid. *Biochimica et*  
683 *Biophysica Acta*, *1674*, 205–214.
- 684 Kragh-Hansen, U. (1990). Structure and ligand binding properties of human serum  
685 albumin. *Danish Medical Bulletin*, *37*, 57–84.
- 686 Liu, Z., Zheng, X., Yang, X., Wang, E., & Wang, J. (2009). Affinity and specificity of  
687 levamlodipine–human serum albumin interactions: Insights its carrier  
688 function. *Biophysical Journal*, *96*, 3917–3925.
- 689 Luisi, I., Pavan, S., Fontanive, G., Tossi, A., Benedetti, F., Sgarra, R., et al. (2013). An  
690 albumin-derived peptide scaffold capable of binding and catalysis. *PLoS One*, *8*,  
691 e56469.
- 692 Min, J., Meng-Xia, X., Dong, Z., Yuan, L., Xiao-Yu, L., & Xing, C. (2004). Spectroscopic  
693 studies on the interaction of cinnamic acid and its hydroxyl derivatives with  
694 human serum albumin. *Journal of Molecular Structure*, *692*, 71–80.
- 695 Monteiro, M., Farah, A., Perrone, D., Trugo, L. C., & Donangelo, C. (2007). Chlorogenic  
696 acid compounds from coffee are differentially absorbed and metabolized in  
697 humans. *Journal of Nutrition*, *137*, 2196–2201.
- 698 Nagy, K., Redeuil, K., Williamson, G., Rezzi, S., Dionisi, F., Longet, K., et al. (2011).  
699 First identification of dimethoxycinnamic acids in human plasma after coffee  
700 intake by liquid chromatography–mass spectrometry. *Journal of*  
701 *Chromatography A*, *1218*, 491–497.
- 702 Nardini, M., Cirillo, E., Natella, F., & Scaccini, C. (2002). Absorption of phenolic acids  
703 in humans after coffee consumption. *Journal of Agricultural and Food Chemistry*,  
704 *50*, 5735–5741.
- 705 Navarini, L., Colomban, S., Lonzarich, V., Rivetti, D., Brollo, G., & Suggi-Liverani, F.  
706 (2008). *Hyper Espresso Coffee Extraction: Adding Physics to Chemistry*. *22nd*  
707 *International Studies on Coffee Science, Proceedings*, Campinas (SP, Brazil):296–  
708 309.
- 709 Olthof, M. R., Hollman, P. C. H., & Katan, M. B. (2001). Chlorogenic acid and caffeic  
710 acid are absorbed in humans. *Journal of Nutrition*, *131*, 66–71.
- 711 Pal, S., & Saha, C. (2014). A review on structure-affinity relationship of dietary  
712 flavonoids with serum albumins. *Journal of Biomolecular Structure and Dynamics*,  
713 *32*, 1132–1147.
- 714 Pantusa, M., Sportelli, L., & Bartucci, R. (2012). Influence of stearic acids on  
715 resveratrol–HSA interaction. *European Biophysics Journal*, *41*, 969–977.
- 716 Renouf, M., Guy, P. A., Marmet, C., Fraerinf, A. L., Longet, K., Moulin, J., et al. (2010).  
717 Measurement of caffeic and ferulic acid equivalents in plasma after coffee  
718 consumption: Small intestine and colon are key sites for coffee metabolism.  
719 *Molecular Nutrition & Food Research*, *54*, 760–766.
- 720 Scholz, B. M., & Maier, H. G. (1990). Isomers of quinic acid and quinide in roasted  
721 coffee. *Zeitschrift für Lebensmittel-Untersuchung und -Forschung*, *190*, 132–134.
- 722 Schrader, K., Kiehne, A., Engelhardt, U. H., & Maier, H. G. (1996). Determination of  
723 chlorogenic acids with lactones in roasted coffee. *Journal of the Science of Food*  
724 *and Agriculture*, *71*, 392–398.
- 725 Skrt, M., Benedik, E., Podlipnik, C., & Ulrih, N. P. (2012). Interactions of different  
726 polyphenols with bovine serum albumin using fluorescence quenching and  
727 molecular docking. *Food Chemistry*, *135*, 2418–2424.
- 728 Sinisi, V., Boronová, K., Colomban, S., Navarini, L., Berti, F., & Forzato, C. (2013).  
729 Synthesis of mono, di and tri-3,4-dimethoxycinnamoyl-1,5- $\gamma$ -quinides.  
730 *European Journal of Organic Chemistry*. <http://dx.doi.org/10.1002/ejoc.201301657>.
- 731 Sudlow, G., Birkett, D. J., & Wade, D. N. (1975a). The characterization of two specific  
732 binding sites on the human serum albumin. *Molecular Pharmacology*, *11*,  
733 824–832.
- 734 Sudlow, G., Birkett, D. J., & Wade, D. N. (1975b). Spectroscopic techniques in the  
735 study of protein binding. A fluorescence technique for the evaluation of the  
736 albumin binding and displacement of warfarin and warfarin–alcohol. *Clinical*  
737 *and Experimental Pharmacology and Physiology*, *2*, 129–140.
- 738 Varshney, A., Sen, P., Ahmad, E., Rehan, M., Subbaro, N., & Khan, R. H. (2010). Ligand  
739 binding strategies to human serum albumin: How can the cargo be utilized?  
740 *Chirality*, *22*, 77–87.
- 741 Yang, F., Yue, J., Ma, L., Ma, Z., Li, M., Wu, X., et al. (2012). Interactive associations of  
742 drug–drug and drug–drug–drug with IIA subdomain of human serum albumin.  
743 *Molecular Pharmaceutics*, *9*, 3259–3265.
- 744
- 745